OXFORD

Human Molecular Genetics, 2015, Vol. 24, No. 18 5198–5210

doi: 10.1093/hmg/ddv241
Advance Access Publication Date: 29 June 2015
Original Article

ORIGINAL ARTICLE

Increased neuronal PreP activity reduces Aβ accumulation, attenuates neuroinflammation and improves mitochondrial and synaptic function in Alzheimer disease's mouse model

Du Fang[1], Yongfu Wang[1], Zhihua Zhang[1,2], Heng Du[1], Shiqiang Yan[3], Qinru Sun[1], Changjia Zhong[1], Long Wu[1], Jhansi Rani Vangavaragu[1], Shijun Yan[1], Gang Hu[1], Lan Guo[1], Molly Rabinowitz[3], Elzbieta Glaser[4], Ottavio Arancio[3], Alexander A. Sosunov[5], Guy M. McKhann[5], John Xi Chen[6] and Shirley ShiDu Yan[1,*]

[1]Department of Pharmacology and Toxicology, Higuchi Bioscience Center, School of Pharmacy, University of Kansas, Lawrence, KS 66047, USA, [2]School of Life Sciences, Beijing Normal University, Beijing 100871, China, [3]Taub Institute for Research on Alzheimer's disease and the Aging Brain, New York, NY 10032, USA, [4]Department of Biochemistry and Biophysics, Stockholm University, Stockholm, Sweden, [5]Department of Neurosurgery, Physicians & Surgeons College of Columbia University, New York, NY 10032, USA and [6]Department of Neurology, Memorial Sloan-Kettering Cancer Center, 1275 York Avenue, New York, NY 10065, USA

*To whom correspondence should be addressed at: Departments of Pharmacology and Toxicology and Higuchi Bioscience Center, School of Pharmacy, University of Kansas, 2099 Constant Avenue, Lawrence, KS 66047, USA. Tel: +1 7858643637; Email: shidu@ku.edu

Abstract

Accumulation of amyloid-β (Aβ) in synaptic mitochondria is associated with mitochondrial and synaptic injury. The underlying mechanisms and strategies to eliminate Aβ and rescue mitochondrial and synaptic defects remain elusive. Presequence protease (PreP), a mitochondrial peptidasome, is a novel mitochondrial Aβ degrading enzyme. Here, we demonstrate for the first time that increased expression of active human PreP in cortical neurons attenuates Alzheimer disease's (AD)-like mitochondrial amyloid pathology and synaptic mitochondrial dysfunction, and suppresses mitochondrial oxidative stress. Notably, PreP-overexpressed AD mice show significant reduction in the production of proinflammatory mediators. Accordingly, increased neuronal PreP expression improves learning and memory and synaptic function *in vivo* AD mice, and alleviates Aβ-mediated reduction of long-term potentiation (LTP). Our results provide *in vivo* evidence that PreP may play an important role in maintaining mitochondrial integrity and function by clearance and degradation of mitochondrial Aβ along with the improvement in synaptic and behavioral function in AD mouse model. Thus, enhancing PreP activity/expression may be a new therapeutic avenue for treatment of AD.

Received: April 9, 2015. **Revised:** June 11, 2015. **Accepted:** June 22, 2015

Introduction

Mitochondrial and synaptic dysfunctions are the early pathological features of Alzheimer's disease-affected brain. Amyloid-β (Aβ) peptide has deleterious effects on mitochondrial functions and contributes to energy failure, respiratory chain impairment, neuronal apoptosis and generation of reactive oxygen species (ROS) in Alzheimer disease (AD) brain tissue. Emerging evidence demonstrates a pathological role of intra-mitochondrial Aβ in AD pathogenesis (1–11). Aβ progressively accumulates in mitochondria of the AD brain and several transgenic (Tg) AD mouse models overexpressing Aβ; such accumulation is associated with mitochondrial and neuronal malfunction in AD. Aβ transports directly into mitochondria via translocase of the outer membrane (TOM) machinery (12), receptor for advanced glycation end-products (RAGE) (13) or endoplasmic reticulum (ER)-mitochondrial cross-talk (14). Mitochondrial Aβ may also be locally produced via mitochondria-localized γ-secretase (15,16). Accumulation of mitochondrial Aβ precedes extra-cellular Aβ deposition in the AD brain and increases with age, which is associated with early onset of synaptic loss and mitochondrial oxidative damage (2,7,17). Interaction of mitochondrial Aβ with mitochondrial proteins exacerbates Aβ-induced neuronal stress (6,8,18). Recent studies indicate that mitochondria are also involved in promoting chronic inflammation and leading to cell death (19). Thus, accumulation of Aβ in mitochondria may be an important mechanism leading to neuronal perturbation in AD. Strategies to reduce Aβ levels in mitochondria could open a new avenue for preventing deterioration of mitochondrial function and halting AD progression.

Presequence protease (PreP), is a specific mitochondrial peptidasome, localized in mammalian mitochondrial matrix (20). PreP normally degrades targeting peptides, presequences, which are cleaved off in mitochondria after completion of protein import and other unstructured peptides up to 70 amino acid residues in length (21). Thus, PreP is a key player in maintenance of mitochondrial health and integrity. *In vitro* study by Falkevall *et al*. showed that PreP can degrade various Aβ peptides and is responsible for clearance of mitochondrial Aβ (20,22). PreP proteolytic activity is significantly reduced in Aβ-affected brain mitochondria from AD-affected brain and AD Tg mouse models (22), which is negatively correlated to mitochondrial Aβ accumulation. Accordingly, Aβ-enriched mitochondria have higher levels of oxidative stress and lower levels of activity of cytochrome c oxidase (CCO) (22). We therefore propose that impaired PreP protease function contributes to chronic mitochondrial Aβ accumulation and resultant amyloid pathology as seen in AD-affected brain, including mitochondrial and synaptic degeneration.

The present study is to address the following unexplored questions: Does PreP activity contribute to mitochondrial Aβ accumulation *in vivo* AD mouse model? If Aβ-loaded mitochondria have increased levels of PreP, will the mitochondrial pool of Aβ decrease, resulting in improved mitochondrial and neuronal function? Does PreP-involved mitochondrial function link to synaptic and cognitive function? Using newly created Tg mice with neuronal expression of human PreP and inactive mutant form of PreP without its proteolytic activity as a control, we comprehensively analyzed the effects of neuronal PreP on synaptic mitochondrial amyloid pathology, mitochondrial function, inflammation, synaptic plasticity and cognition in a Tg AD mouse model that overexpresses neuronal Aβ. We provide substantial evidence *in vivo* that PreP-dependent clearance of mitochondrial Aβ improves synaptic and behavioral functions in AD mouse models.

Results

Generation and characterization of Tg mice overexpressing neuronal PreP

To evaluate the effect of PreP activity in Aβ-rich environment relevant to the pathophysiology of AD, we first created Tg mice with selective expression of human PreP in neurons under the control of Thy-1 promoter (PreP mice, Supplementary Material, Fig. S1A). We also generated control mice with an inactive mutant PreP (20) in which the catalytic base Glu78 in the inverted zinc-binding motif is replaced by Gln (PE mice) to validate the role of PreP proteolytic activity (Supplementary Material, Fig. S1B and C). PreP expression was determined in neuronal mitochondrial (Supplementary Material, Fig. S1C), and cytosolic fraction isolated from the Tg mice (Supplementary Material, Fig. S1D). PreP expression levels were significantly increased in neuronal mitochondrial fraction (Supplementary Material, Fig. S1C), but not in cytosolic fraction (Supplementary Material, Fig. S1D), from PreP and PE mice as compared with non-transgenic (nonTg) mice, demonstrating that expressed PreP specifically resides in mitochondria. PreP expression levels in PreP mice were comparable to that of PE mice. Immunostaining of brain section with PreP antibody verified that PreP was increased in cortical neurons of both PreP and PE mice (Supplementary Material, Fig. S1E, green). To confirm the localization of PreP in mitochondria, we performed confocal and electron microscopic studies in brain tissues. Using confocal microscopy, increased expression of PreP (Supplementary Material, Fig. S1E, green) is colocalized with cytochrome c oxidase (CCO, red), a mitochondrial protein, in PreP and PE mice (Supplementary Material, Fig. S1E, merge yellow). Immunogold electron microscopy with gold-conjugated antibody to PreP further verified that specific PreP gold particles were identified in pre- and post-synaptic mitochondria of PreP mice (Supplementary Material, Fig. S1F). Accordingly, PreP proteolytic activity was significantly increased in PreP-enriched cortical mitochondria as shown by measuring substrate V degradation (Supplementary Material, Fig. S1G) and the enhanced ability for degrading exogenous Aβ compared with those from nonTg or PE mitochondria (Supplementary Material, Fig. S1H). As expected, there was no difference in PreP proteolytic activity between nonTg and PE mice.

To determine the effects of PreP on Aβ-associated mitochondrial defects, Aβ accumulation and cognitive functions *in vivo* AD mouse model, PreP or PE mice were crossed with single Tg mAPP mice to generate double Tg mAPP/PreP or mAPP/PE mice overexpressing human Aβ and human PreP in neurons. Transgenic mAPP mice overexpressing human Aβ were previously well characterized with respect to mitochondrial function and neuropathological, behavioral and electrophysiological parameters (5,6,8,23–26). Following double immunostaining of PreP and CCO with confocal microscope, we observed increased PreP expression in cortical neurons in mAPP/PreP and mAPP/PE brain (Supplementary Material, Fig. S2A, green); both images were identically overlaid (Supplementary Material, Fig. S2A, yellow). Further, electron microscopy revealed that PreP immunogold particles were located in pre- and post-synaptic mitochondria of mAPP/PreP and mAPP/PE mice (Supplementary Material, Fig. S2B). These data verify that PreP protein is correctly targeted to mitochondria in PreP-expressed mAPP mice.

Increased neuronal PreP proteolytic activity attenuates synaptic mitochondrial Aβ accumulation

The mitochondrial PreP extracted from mAPP/PreP mice significantly enhanced degradation of Aβ compared with those from

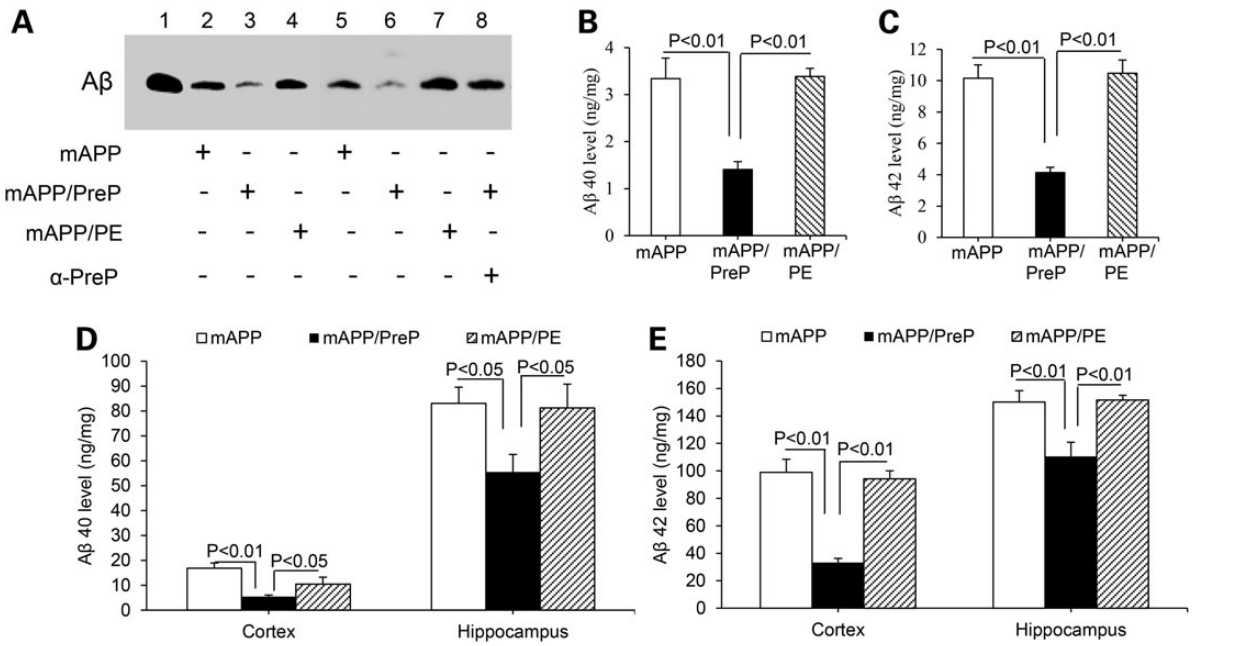

Figure 1. Effects of PreP overexpression and activity on mitochondrial and cerebral Aβ load in mAPP mice. (**A**) PreP activity for degrading Aβ. PreP-enriched mitochondria from APP/PreP mice degraded significant amount Aβ1-42 as shown by less Aβ immunoreactive band, compared with mitochondria from APP or APP/PE mice. The addition of anti-PreP antibody to mitochondrial PreP protein extracted from APP/PreP mitochondria completely blocked degradation of Aβ (lane 8). Lane 1 denotes biotin-Aβ (10 ng) as a positive control. (**B–E**) Aβ levels in synaptic mitochondrial fractions (B and C) and cerebral cortex and hippocampus (D and E) from the indicated Tg mice were measured by ELISA. $N = 6–14$ mice per group.

mAPP and mAPP/PE mice (Fig. 1A). The addition of PreP antibody to the mitochondrial lysates from APP/PREP cortical mitochondria containing PreP protein blocked degradation of exogenous Aβ by neutralizing PreP antibody with its antigen PreP protein (Fig. 1A, lane 8). As expected, there was no difference in PreP proteolytic activity between mAPP and mAPP/PE mice (Fig. 1A). This indicates that Tg mice overexpressing neuronal mitochondrial PreP in Aβ-rich AD mice are appropriate models for the investigation of role of PreP in mitochondrial amyloid pathology and synaptic function.

Next, we examined the effect of PreP overexpression on mitochondrial Aβ accumulation. The synaptic mitochondria were isolated from the cortex of mAPP and mAPP/PreP mice, aged 12 months, an age at which marked mitochondrial Aβ accumulation and mitochondrial defects are observed. The mitochondrial pool of Aβ40 and Aβ42 was significantly reduced in mAPP/PreP mice compared with single mAPP mice (Fig. 1B and C). Interestingly, Aβ40 and Aβ42 levels were also significantly lower in cerebral cortex and hippocampus of mAPP/PreP compared with mAPP mice (Fig. 1D and E). Aβ immunoreactive plaque load was also reduced in the brain of mAPP/PreP mice but not in mAPP/PE mice (Supplementary Material, Fig. S2C and D). Human Aβ was not found in mitochondrial fraction and cerebral cortex of Tg PreP, PE and nonTg mice (data not shown). These data indicate that increased PreP expression attenuates both intra-mitochondrial and overall cerebral Aβ levels.

Increased neuronal PreP expression ameliorates synaptic mitochondrial dysfunction

To determine whether reducing mitochondrial Aβ improves mitochondrial function. We first evaluated baseline mitochondrial respiratory function by measuring mitochondrial oxygen consumption and CCO enzymatic activity. The mitochondrial respiration control ratio (RCR) is an index of mitochondrial coupling, which reflects the efficacy of mitochondrial oxidative phosphorylation. Synaptic mitochondria from mAPP mice underwent a significant reduction in RCR compared with nonTg mice (Fig. 2A), whereas the RCR of mAPP/PreP mitochondria was significantly recovered (Fig. 2A). Similarly, CCO enzyme activity in synaptic mitochondria of mAPP mice was decreased compared with nonTg littermate controls, whereas CCO activity was completely recovered in mAPP/PreP mitochondria (Fig. 2B). CCO activity and respiratory rates in nonTg mitochondria were comparable to PreP mitochondria, suggesting that increased PreP expression does not alter mitochondrial respiratory function under physiologic conditions. We then assessed brain mitochondrial energy metabolism by measuring brain ATP levels. Brain samples from mAPP mice had significantly reduced ATP levels compared with nonTg mice. In contrast, declines in ATP levels were largely reversed in mAPP/PreP mice (Fig. 2C).

Increased PreP activity reduce oxidative stress

Because mitochondria are a major resource of ROS generation, we next assessed whether increased PreP expression attenuates ROS production in Aβ-affected brain. Consistent with our previous results (8), brains of mAPP mice demonstrated remarkably increased MitoSox-Red, an indicator of mitochondrial superoxide, in terms of staining intensity of MitoSox-positive cells in hippocampus and cortex, indicating increased ROS accumulation in Aβ-loaded mitochondria. In contrast, MitoSox-Red signal was significantly suppressed in hippocampus and cortex of mAPP/PreP mice (Fig. 2D and E). There are no significant differences of MitoSox signals among nonTg, PreP and PE group of mice (Supplementary Material, Fig. S3). To further confirm the cerebral oxidative stress in mAPP mice, we quantitatively measured the intra-cellular ROS levels by a highly specific election

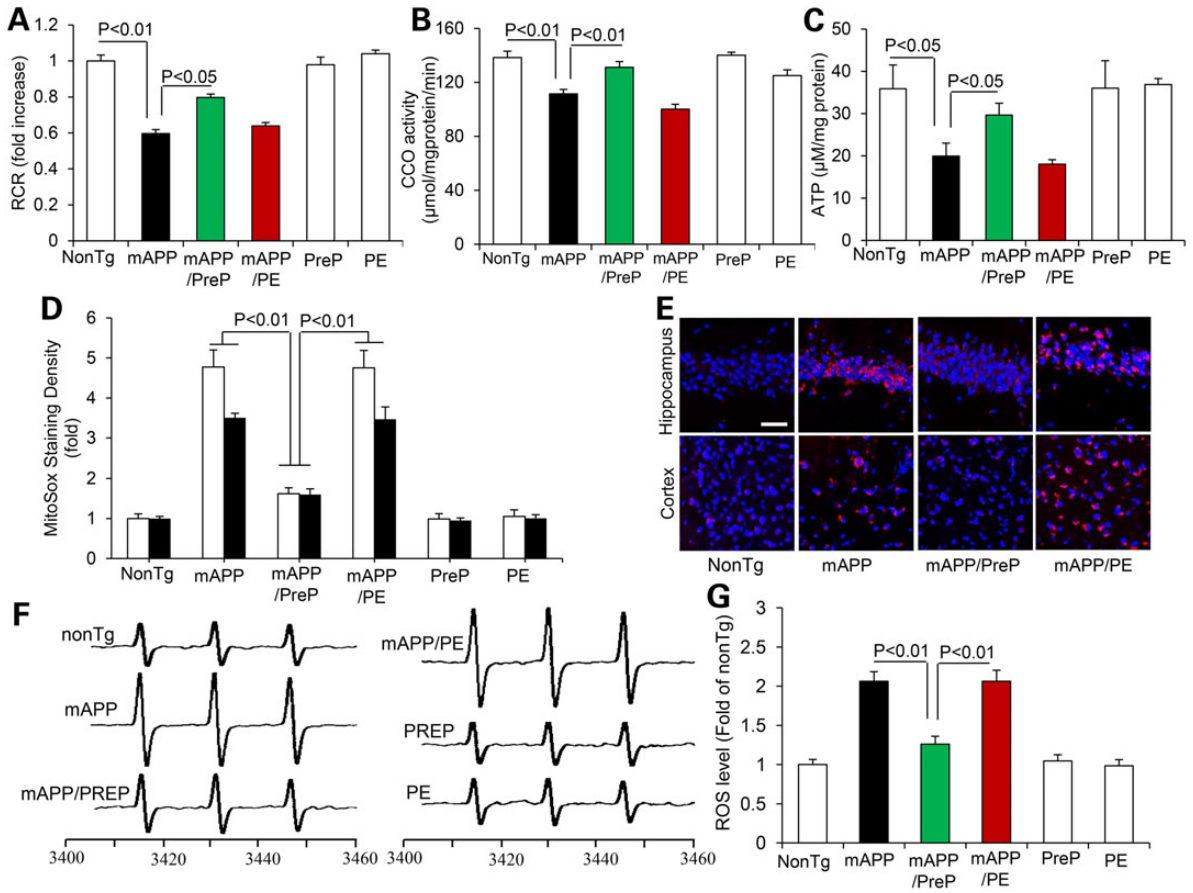

Figure 2. Effect of PreP overexpression and activity on synaptic mitochondrial function in mAPP mice. Synaptic mitochondria were isolated from the indicated old Tg mice at 12–13 months of age. We measured mitochondrial respiratory control ratio (RCR, **A**) and CCO activity (**B**). There were no significant differences in RCR and CCO activity when comparing mAPP and mAPP/PE mice. $N = 4–13$ mice per group. (**C**) ATP levels in brain cortex tissue of the indicated Tg mice. $N = 4–7$ mice per group. (**D** and **E**) Quantification of intensity of MitoSox staining (D) and the representative image of MitoSox signals (E) in hippocampus and cortex of the indicated Tg miceScale bar = 50 μm. (**F** and **G**) Representative spectra of EPR. The peak height in the spectrum indicates levels of ROS. (G) Quantification of EPR spectra in the indicated Tg mice. Data are expressed as fold-increase relative to nonTg mice. $N = 3–6$ mice per group.

paramagnetic resonance (EPR) spectroscopy in cortex. Compared with nonTg mice, the intra-cellular ROS levels were significantly elevated in mAPP brain, which was largely abolished in mAPP/PreP mice but not in mAPP/PE mice (Fig. 2F and G). Together, these data suggest that increased PreP expression/activity attenuates mitochondrial ROS production and accumulation.

Effects of PreP on proinflammatory mediators in mAPP/PreP mice

Because mitochondria play an important role in proinflammatory signaling and dysfunctional mitochondria could potentiate inflammation and thus promotes cell death (27), we hypothesize that protective effect of PreP on mitochondrial function may lessen inflammation in Aβ-affected brain. To test this concept, we first assessed expression levels of proinflammatory cytokines and chemokines in cortical tissue. Consistent with our previous studies (28), mAPP mice showed a significant increase in cytokines (TNF-α and IL-1β) and chemokine MCP-1 compared with nonTg control mice. Notably, mAPP/PreP mice largely attenuated the production of these proinflammatory mediators (Fig. 3A–C). Given that RAGE serves as an important cell-surface receptor-mediating chemotactic and inflammatory in response to Aβ and other proinflammatory ligands, we evaluated RAGE expression levels as well as microglial markers (CD4 and CD11b) in the brain. mAPP/PreP mice showed significant suppression of RAGE expression in addition to CD11b and CD4 as compared with mAPP mice (Fig. 3D–F). These results suggest the role of PreP in Aβ-mediated inflammation in addition to mitochondrial dysfunction.

Increased expression of neuronal PreP improves synaptic and behavioral function

Given that synaptic mitochondria are vital for maintenance of synaptic function and transmission, we examined synaptic transmission under basal conditions and during LTP, a form of synaptic plasticity that is widely studied as a cellular model for learning and memory. Hippocampal slices from 12 to 13-month-old nonTg control, PE and PreP mice showed similar levels of basal neurotransmission (field-excitatory post-synaptic potential, fEPSPs, Supplementary Material, Fig. S4A) and LTP in the CA1 stratum radiatum (Supplementary Material, Fig. S4B). However, basal synaptic transmission (BST) was significantly reduced in mAPP and mAPP/PE CA1 neurons compared with nonTg and mAPP/PreP CA1 neurons (Supplementary Material, Fig. S4C). LTP recorded from CA1 neuron was significantly declined in mAPP mice compared those from nonTg mice. Slices from

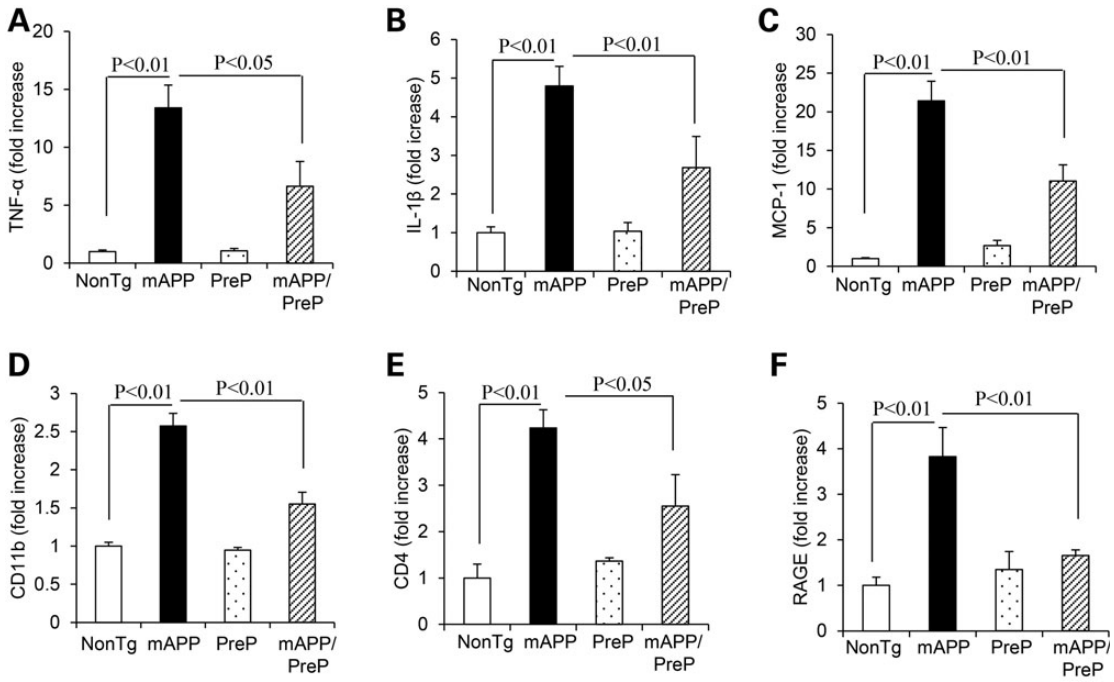

Figure 3. Effect of PreP overexpression on induction of proinflammatory cytokines and RAGE expression in Tg brains. Quantitative real-time PCR analysis of cytokines (TNF-α, **A**; IL-1β, **B** and MCP-1, **C**), microglial makers (CD11b, **D**; and CD4, **E**) and RAGE (**F**) of total RNA extracted from cerebral cortex of the indicated Tg mice at 12–14 months of age (4–6 mice/group).

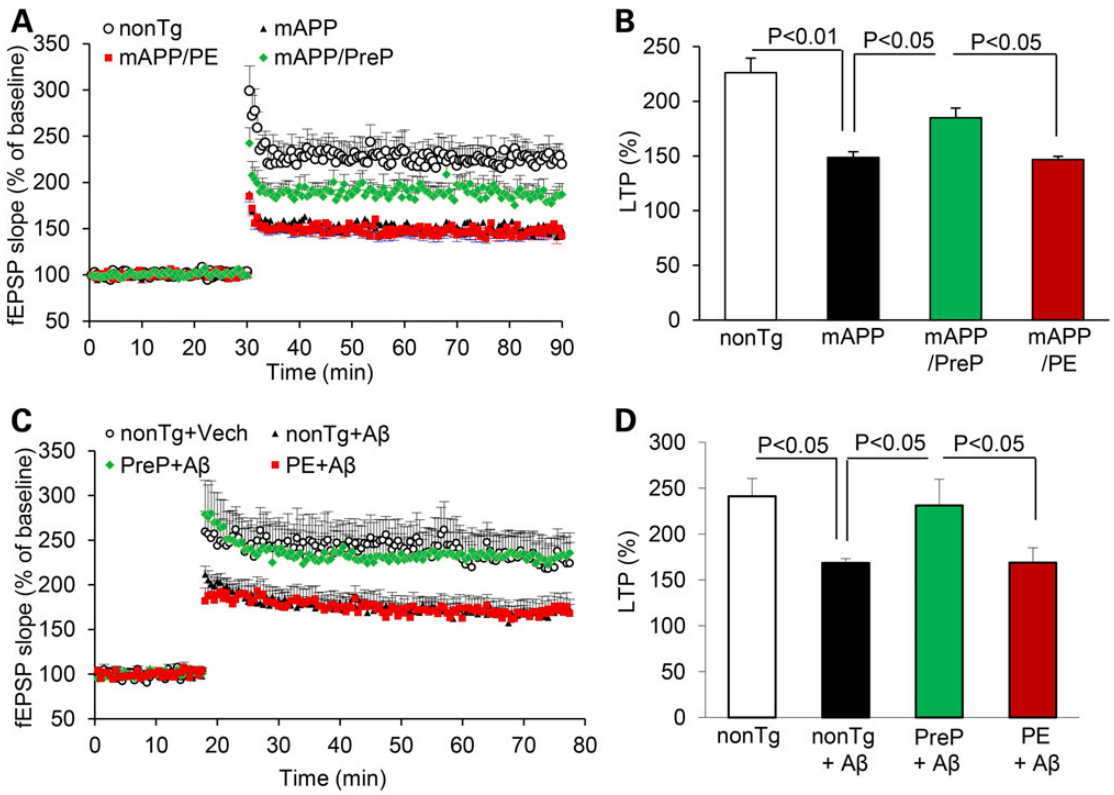

Figure 4. Effect of PreP overexpression and activity on LTP impairment. LTP was recorded in hippocampal slices of the indicated Tg mice (12–13 months of age). Slices from 12 to 13 months old mAPP mice showed a reduced LTP compared with nonTg slices. MAPP/PreP slices had significantly increased LTP compared with mAPP slices (**A** and **B**). (**C** and **D**) Effect of PreP on Aβ-induced LTP decline. Hippocampal slices from the indicated Tg mice were treated with vehicle or Aβ (200 nM), and then recorded CA1 LTP for 120 min. Data are presented as mean ± SE. *N* = 8–12 slices per group.

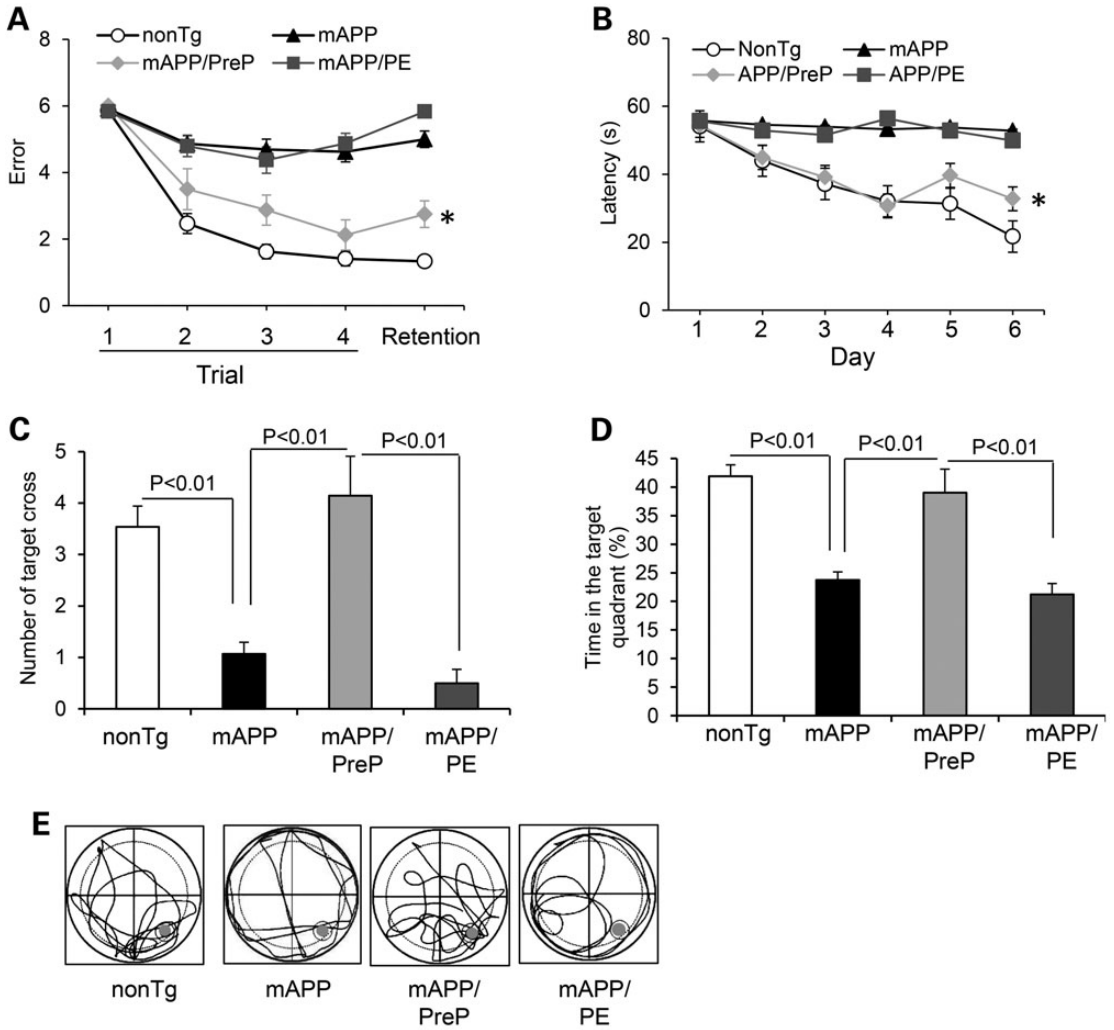

Figure 5. Effect of PreP overexpression and activity on learning memory in mAPP mice. (**A**) Radial water maze test in the indicated Tg mice at 12–13 months of age. *$P < 0.05$ versus Tg mAPP or mAPP/PE mice. $N = 8–10$ mice per group. (**B–E**). Results of the MWM test showed the average latency to escape to locate the hidden platform during each day of training sessions (B), *$P < 0.05$ compared with Tg mAPP or Tg mAPP/PE mice, the mean number of mice crossing the target during probe trials (C), and time spent in the quadrant where the hidden platform is located (D). Tg mAPP and mAPP/PE mice showed much less preference for the target quadrant compared with nonTg mice. MAPP/PreP mice demonstrated an increase in the percentage of time spent in the target quadrant compared with mAPP or mAPP/PE mice. (E) Pattern of representative searching traces for the indicated Tg mice in search of the target. $N = 8–15$ mice per group.

mAPP/PreP mice showed a largely restored LTP, but no such protection was found in mAPP/PE mice compared with mAPP mice (Fig. 4A and B). To determine the direct effect of PreP on Aβ-induced LTP deficit, we recorded LTP in hippocampal slices from PreP, PE and control mice treated with Aβ. We found similar potentiation levels in PreP and PE slices compared with nonTg slices in the presence of vehicle. LTP was significantly reduced in control slices following treatment with 200 nM oligomeric Aβ42. However, PreP hippocampal slices were significantly resistant to Aβ-mediated deficits in LTP (Fig. 4C and D). Notably, PE slices were not protected from Aβ-mediated LTP reduction. Taken together, these data demonstrate that increased PreP expression/activity significantly alleviates synaptic damage in Aβ-rich brain.

We next examined whether PreP protection of synaptic activity also improves cognitive function. Mice were first subjected to a spatial learning and memory test using a radial arm water maze. For spatial learning and memory tasks, single PreP, PE, and nonTg mice found the platform with 1–2 errors (Supplementary Material, Fig. S5A), showing good memory. Tg mAPP mice had 5–6 errors, whereas mAPP/PreP mice made significantly fewer errors (2–3 errors). In a retention memory test, mAPP/PreP mice showed significantly improved spatial reference memory conducted 30 min after trial (Fig. 5A). We further assessed the spatial reference memory and target searching strategy using a Morris Water Maze (MWM). Compared with mAPP mice, mAPP/PreP mice revealed a shorter latency to locate the hidden platform during the training session (Fig. 5B) and increased the number of times crossing the target (Fig. 5C) and time in the target quadrant (Fig. 5D) in the recording period. In the Probe test, mAPP/PreP mice revealed an increased search activity in the quadrant where the hidden platform was located compared with mAPP mice (Fig. 5E). These results demonstrate that mAPP/PreP retained a better searching strategy. There was no significant difference in latency among PreP, PE and nonTg mice (Supplementary Material, Fig. S5B), indicating no effect of PreP overexpression on baseline spatial reference memory. The Tg mice among tested groups had similar swimming speed by the visual swimming speed test

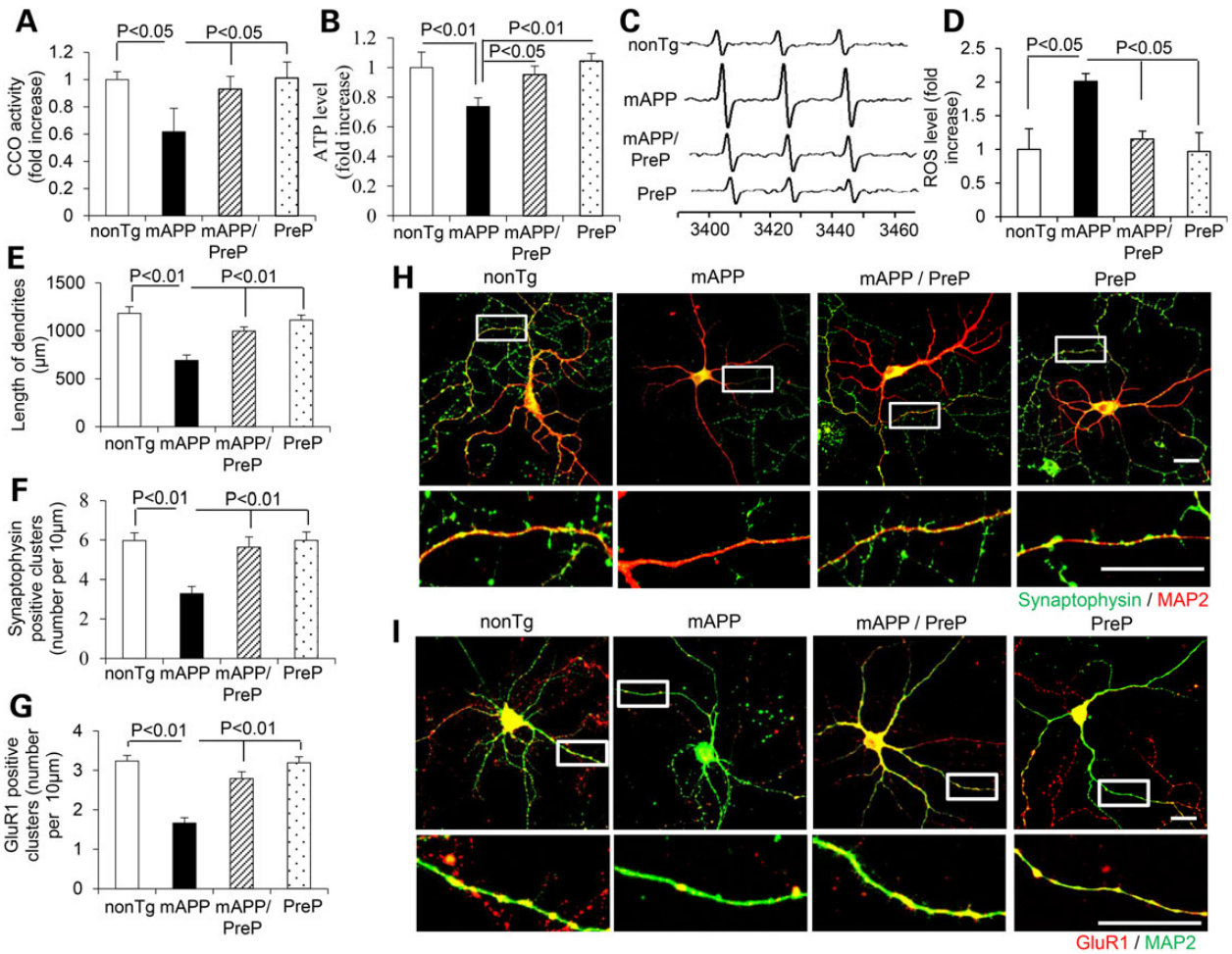

Figure 6. Effect of neuronal PreP on mitochondrial function, ROS and synaptic density in cultured AD neurons. Complex IV/CCO activity (**A**), ATP levels (**B**) and cellular ROS (**C** and **D**) were measured in hippocampal neurons derived from the indicated Tg mice. Representative EPR spectra (C) and quantification (D) for ROS signals in the indicated groups of cells. Data are expressed as fold-increase relative to nonTg neurons. (**E–I**) Effect of PreP on length and synaptic density of neuronal dendrites. Hippocampal culture neurons from the indicated Tg mice *in vitro* day 12 were stained with MAP2 (a marker for dendrites, H and I) and Syn (pre-synaptic marker, green, H) or GluR1 (post-synaptic marker, red, I). Quantification of a total length of dendrites (E), number of synaptophysin-positive clusters (F) and GluR1-positive clusters (G) per micron of dendrite length was performed in the indicated groups of cells. (H) The representative staining images for synaptophysin (green) and MAP2 (red), or for (I) GluR1 (red) and MAP2 (green) in the indicated groups of cells. The lower panels of H and I are enlarged images corresponding to above framed images.

(Supplementary Material, Fig. S5C and D). Thus, the observed difference in spatial learning and memory is a result of defects in cognition but not motility or altered motivation. These data indicate that increased neuronal PreP expression and activity improves learning and memory in mAPP mice.

PreP proteolytic activity is essential for clearance of mitochondrial Aβ resulting in improved cognitive function

To further validate the role of PreP activity, we examined the inactive mutant form of PreP, which lacks PreP proteolytic activity on mitochondrial Aβ levels, synaptic mitochondrial function, synaptic plasticity and learning and memory. Compared with mAPP/PreP mice, we did not observe any protective effects on human Aβ levels in mAPP/PE mitochondria and cerebral cortex in which mitochondrial Aβ levels were comparable to single mAPP mice (Fig. 1B–E). As a result, there were no protective effects of mAPP/PE mice on RCR, CCO activity, ATP levels and mitochondrial ROS generation and accumulation (Fig. 2A–G). Similarly, mAPP/PE mice did not reverse defects in LTP and behavior observed in mAPP mice (Figs. 3–5). These results suggest that PreP proteolytic activity is essential for degradation and clearance of mitochondrial Aβ accumulation and maintenance of mitochondrial and synaptic function.

Effect of PreP on mitochondrial function and synaptic density *in vitro* cultured AD neurons

To determine the direct effect of neuronal PreP on Aβ-induced mitochondrial dysfunction and synaptic damage, we first analyzed mitochondrial function by measuring CCO activity and ATP levels in cultured hippocampal neurons derived from nonTg, mAPP, mAPP/PreP and PreP mice. Neurons from mAPP mice revealed significant decline in CCO activity and ATP levels compared with nonTg neurons (Fig. 6A and B). The mAPP/PreP neurons reversed the deficits of CCO activity and ATP. Similarly, ROS levels in mAPP/PreP neurons were significantly lower than mAPP neurons (Fig. 6C and D). To assess the effect of PreP on synaptic alterations, we measured total length and synaptic density of neuronal dendrites. The mAPP/PreP neurons displayed an increase in length of dendrites compared with mAPP neurons

(Fig. 6E). Synaptic density was quantified by measuring synaptophysin (Syn, pre-synaptic marker) and glutamate receptor 1 (GluR1, post-synaptic marker)-positive clusters attaching to dendrites labeled with MAP2. The mAPP/PreP neurons increased both pre- and post-synaptic densities compared with mAPP neurons (Fig. 6F–I). These results suggest that increased PreP expression rescues Aβ-induced mitochondrial dysfunction and loss of synapses.

Discussion

In the present studies, we provide substantial evidence of the beneficial effect of PreP expression and activity, a mitochondrial Aβ scavenger, on rescuing AD-like mitochondrial and synaptic pathology as well as cognitive impairment in a Tg AD mouse model. Our results illustrate that increased expression and activity of neuronal PreP significantly reduced mitochondrial Aβ load, improved mitochondrial function and synaptic plasticity and strength. As a result, cognitive function decline in AD mice was substantially attenuated by PreP overexpression. Notably, there is no protection in AD mice expressing comparable levels of non-functional mutant human PreP on Aβ-associated mitochondrial and synaptic pathology, suggesting that PreP proteolytic activity is required for degradation and clearance of mitochondrial Aβ. Furthermore, we unexpectedly found that increased PreP expression in mAPP mice significantly attenuates production of proinflammatory mediators.

Emerging evidence indicates that mitochondria are a target organelle of Aβ invasion. In AD patients and mouse models of AD, Aβ progressively accumulates in mitochondria and penetrates through mitochondrial membrane via mitochondrial protein transport machinery (29,30). The accumulation of Aβ in mitochondria is associated with increased ROS production, decreased mitochondrial membrane potential and ATP production, reduced mitochondrial calcium handling capacity, release of mitochondrial pro-apoptotic factors and defects in mitochondrial dynamics and motility (6,11,18,31–35). Importantly, early accumulation of Aβ occurs in mitochondria at synapses, which might make synaptic mitochondria more vulnerable to Aβ toxicity (7). Mitochondria maintain synaptic ion homeostasis and synaptic plasticity through producing ATP and controlling local Ca^{2+} concentration. Aβ accumulation causes the impairment of mitochondrial transport and altered mitochondrial dynamics (9,18,36). Aberrant mitochondrial function is associated with Aβ-altered synaptic structure and function such as loss of synapses and dendritic spines, pre- and post-synaptic proteins and reduction of LTP (6,8,25,26,37,38). The early synaptic mitochondrial damage suggests that AD neurons may have already suffered harm for years, which may help explain the limitations to current amyloid hypothesis. Thus, strategies that suppress/attenuate Aβ-induced mitochondrial toxicity in addition to Aβ levels in the brain and improve cognitive function are critical for preventing and/or halting AD at a very early stage by improving mitochondrial function. Elimination of mitochondrial Aβ load could be an important strategy for rescuing mitochondrial and synaptic alterations.

Over the years, approaches to effectively clear Aβ from brain tissue have been considered as 'holy grail' for treatment of AD. The strategies include to inhibit Aβ production by reducing amyloid precursor protein (APP) production or β-/γ-secretase, and to enhance Aβ clearance and degradation. IDE (insulin-degrading enzyme), a widely expressed extra-cellular zinc-metallopeptidase, regulates both extra-cellular cerebral Aβ peptide and plasma insulin levels *in vivo* (39). A mitochondrial isoform of IDE, which degrades cleaved mitochondrial targeting sequences (40), could involve in degrading and clearing mitochondrial Aβ. While effects of IDE on AD has been supported by both animal models and epidemiological evidences, the mechanisms involved are complex due to its involvement with both extra- and intra-cellular Aβ as well as regulation of insulin metabolism, another possible risk factor of AD. On the contrary to the ubiquitous nature of IDE, PreP, as a specific mitochondrial PreP, was also found to be associated in clearing mitochondrial Aβ. Using confocal and immunogold electron microscopy, we confirmed that PreP protein in PreP-overexpressed Tg mice is exclusively localized in mitochondria. Thus, enhancing PreP proteolytic activity may hold a potential therapeutic strategy for treatment of AD at early stage by accelerating clearance of mitochondrial Aβ and improving mitochondrial and synaptic function (41).

In terms of Aβ and mitochondria, there are several mechanisms through which Aβ gains and accumulates in mitochondria. Generation of Aβ has been demonstrated to occur in the intracellular compartments including ER/Golgi and lysosomes/endosomes, as well as on the cell surface (42–46). In view of the known production of Aβ from APP in ER, ER-produced Aβ releases to cytosol or extra-cellular space via Gogli and lysosomes/endosomes transport pathway. The extra-cellular Aβ could be internalized by cells and transported into the intra-cellular compartments via RAGE (13) or unknown Aβ carriers. Furthermore, the intra-cellular Aβ, including internally ER-produced Aβ or up-taken from the extra-cellular Aβ, could directly import into mitochondria through translocase of the mitochondrial out membrane (TOM) machinery (12), RAGE (13) or ER/mitochondrial cross-talk via mitochondria-associated membranes (14). The study showing that the treatment of brefeldin A (BFA), an inhibitor of protein transport from ER/intermediate compartment (5), significantly increased mitochondrial Aβ accumulation, suggest the involvement of ER in mitochondrial Aβ accumulation. The detailed mechanisms by which Aβ gains and accumulates in mitochondria will be explored in future studies.

We also unexpectedly observed that increased expression of PreP not only degrades mitochondrial Aβ but also affects a total of brain Aβ levels, suggesting that mitochondrial Aβ is not just a 'pilling over' from extra-cellular aggregation but also having an important regulating effect on the total brain Aβ levels. Given that exogenous or intra-cellular Aβ is capable of direct transport into mitochondria via aforementioned pathways, the mitochondrial pool of Aβ may undergo dynamic changes in different intra-cellular compartments, contributing to the balance of intra-cellular/extra-cellular Aβ accumulation. The underlying mechanisms of regulation of mitochondrial and cerebral pool of Aβ require further investigation.

Intriguingly, enhancing clearance and degradation of mitochondrial Aβ in mAPP/PreP mice attenuate the production of proinflammatory mediators and microglial activation. There are several possible mechanisms underlying PreP/Aβ-mediated neuroinflammation by induction of proinflammatory mediator and activation of microglia. Given that dysfunction or damaged mitochondria can result in excessive inflammation and tissue damage (19,47), possible via overproduction of ROS or cytokine production, we propose that, among other deleterious effects, mitochondrial Aβ accumulation might interfere with normal mitophage and release mitochondria-derived damage-associated molecular patterns (DAMPs) from the injured neurons, leading to increased production of TNF-α, IL-1β and MCP1, the cytokines/chemokines known to be involved in the neuroinflammatory process of AD. Another possible mechanism is via RAGE-dependent signal transduction. RAGE serves as important cell-surface

receptor-mediating chemotactic and inflammatory reaction in response to Aβ and other proinflammatory ligands. RAGE signaling in neurons and microglia is known to promote induction of proinflammatory mediators including cytokine and chemokine, as well as activation of microglia by increased expression of microglial markers (CD4 and CD11) in the Aβ-enriched brain (24,28,48,49). In the present study, we demonstrate that increased neuronal PreP in mAPP mice not only reduced Aβ accumulation in the brain but also remarkably suppressed RAGE expression as compared with mAPP mice. These results suggest the involvement of RAGE in PreP/Aβ-mediated cytokine and chemokine production along with microglial activation as shown in mAPP and mAPP/PreP mice. Our results suggest the role of PreP in mitochondria-inflammation axis in Aβ-mediated mitochondrial and neuronal perturbation.

In summary, we present a new insight into the role of mitochondrial PreP in neuronal mitochondrial Aβ pathology and resultant mitochondrial and synaptic dysfunction relative to Aβ-rich AD mitochondria. We clearly show that increased neuronal human PreP expression and activity in AD model significantly reduce mitochondrial and cerebral Aβ accumulation, suppress the induction of proinflammatory mediators and improve synaptic mitochondrial function. Accordingly, we observe greatly improved synaptic transmission and spatial learning and memory in human disease phenotype of AD mouse model with neuronal PreP overexpression. These data support that the recently identified mitochondrial peptidasome, PreP, functions as a peptide scavenger, clearing off mitochondria of Aβ, and thereby protecting mitochondria against pathogenic peptide intruders. Thus, development of a small molecule PreP agonist (41) to upregulate PreP proteolytic activity that degrades Aβ would represent a novel therapeutic approach to improve mitochondrial and neuronal function by eliminating or at least decreasing steady-state mitochondrial Aβ levels, thereby halting AD progression at the early stage.

Materials and Methods

Generation of Tg PreP mice

Animal studies were approved by the Animal Care and Use Committee of the University of Kansas in accordance with the National Institutes of Health guidelines for animal care. Selective overexpression of human PreP and mutant inactive form of PreP (PE) in mice neurons was achieved under the control of Thy-1 promoter (termed Tg PreP or PE), in view of its previous success in driving overexpression of Tg gene in neurons (24). To generate the Thy1-hPreP construct, we subcloned a full length human PreP coding sequences (AAH05025, gi:13477137) into a Thy1 Tg construct inserted into XhoI site (Supplementary Material, Fig. S1A). Mutant form of hPreP (E107Q) (PE) were constructed using a QuikChange site-directed mutagenesis kit (Stratagene). All constructs were verified by sequencing of human PreP gene.

Tg PreP and PE Tg mice were backcrossed to C57BL6/J mice for 10 times for analysis of expression patterns to eliminate the potential effect of genetic background. Tg PreP or PE mice were identified as bearing the transgene from analysis of tail DNA based on PCR amplification using primers [5′-CCACAGAATCCAAGTCG-3′(forward) and 5′-GTGGAAAATGGATACAGAGT-3′(reverse)] (Supplementary Material, Fig. S1B).

To generate double Tg mice overexpressing PreP and Aβ (Tg mAPP/PreP or mAPP/PE), Tg PreP or PE mice were crossed with Tg mAPP mice that overexpress a human mutant form of APP bearing both the Swedish (K670N/M671L) and the Indiana (V717F) mutations (APPSwInd, J-20 line, obtained from Jackson Lab). Both male and female were used for the described experiments. The investigators were blinded to the mouse genotype in performing experiments.

Synaptic mitochondria preparation

Synaptic mitochondria preparation has been described previously (7,50). Briefly, brain cortices were placed in a 5× volume of ice-cold isolation buffer [225 mM mannitol, 75 mM sucrose, 2 mM K_2PO_4, 0.1% BSA, 5 mM Hepes, 1 mM EGTA (pH 7.2)]. The tissue was homogenized with a Dounce homogenizer (Kontes Glass Co.). The resultant homogenates were centrifuged at 1300*g* for 5 min, and the supernatant was layered on a 3 × 2-ml discontinuous gradient of 15, 23 and 40% (vol/vol) Percoll and centrifuged at 34 000*g* for 8 min. After centrifugation, band 2 (the interface between 15 and 23% containing synaptosomes) and band 3 (the interface between 23 and 40% containing nonsynaptic mitochondria) were removed from the density gradient. The fractions were then resuspended in 20 ml of isolation buffer containing 0.02% digitonin and incubated on ice for 10 min. The suspensions were then centrifuged at 16 500*g* for 15 min. The resulting loose pellets were washed for a second time by centrifugation at 8000*g* for 10 min. Pellets were collected and resuspended in isolation buffer. A discontinuous Percoll density gradient centrifugation was performed as described above for a second time. Band 3 was obtained and resuspended in isolation buffer to centrifuge at 16 500*g* for 15 min. The resultant pellet was washed in isolation buffer at 8000*g* for 10 min. The final synaptic mitochondrial pellet was resuspended in isolation buffer and stored on ice. Protein concentration was determined using the Bio-Rad DC protein assay (BioRad Laboratories).

Cytosol preparation

Brain tissues from the indicated Tg mice were homogenized and subject to a centrifugation at 1300*g* for 5 min to get rid of cell debris. The supernatant was then centrifuged at 10 000*g* for 10 min. The resultant supernatant was subjected to an ultracentrifugation at 100 000*g* for 1.5 h and the supernatant was collected.

Immunofluorescent staining

Brain slices from the indicated Tg mice were subjected to double immunostaining with rabbit anti-PreP IgG antibody (1:2000) and mouse anti-CCO at 4°C overnight followed by the conjugation of goat anti-rabbit Alex488 and goat anti-mouse 594, respectively. The staining was checked and images were taken on a Leica Confocal Microscope.

Electron microscopy

Ultrathin sections were incubated with rabbit anti-PreP IgG antibody (1:2000) overnight at 4°C; this was followed by conjugation of donkey anti-rabbit antibody to colloidal gold (18-nm gold particle) for 2 h at room temperature. Sections were counterstained with uranyl acetate and examined under EM (JEOL 100S) (7).

Measurement of PreP proteolytic activity

We used a fluorescence assay with fluorogenic substrate V (7-methoxycoumarin-4-yl-acetyl-NPPGFSAFK-2, 4-dinitrophenyl, R&D Systems) and measured the kinetics of proteolysis as previously described (41). This peptide contains both the fluorescent group 7-methoxycoumarin and the quenched rgroup2, 4-dinitrophenyl, resulting in fluorescence emission upon cleavage of a

peptide bond between the two groups. Reaction was carried out in the presence of 10 μg mitochondrial hPreP protein in 20 mM HEPES, pH 8.0 with 10 mM MgCl2 mixed with 50 μg Substrate V in a final volume of 250 ml. The hydrolysis of substrate V was measured for 6 min using a fluorometer (SpectraMax Gemini) with excitation and emission wavelengths set at 320 and 405 nm, respectively. Results are shown as the relative fluorescence unit (RFU) as a substrate V degradation rate. The degradation of Aβ for studying PreP proteolytic activity in brain mitochondrial matrix fraction was described previously (22). Briefly, 15 μg isolated matrix PreP protein was incubated with Biotin-labeled Aβ1-42 in a degradation buffer containing 20 mM HEPES-KOH pH 8.0, and 10 mM $MgCl_2$ at 37°C for 2.5 h. The immuno-inactivation was performed by pre-incubating mitochondrial fractions with anti-PreP antibody at 25°C for 2 h before the addition of Biotin-labeled Aβ. Reactions were stopped by the addition of 2× sample buffer and analyzed on NuPAGE 12% Bis–Tris gel (Invitrogen, CA, USA). For analyzing the degradation of Biotin-labeled Aβ1-42 (Biotin-LC-Aβ1-42), the nitrocellulose membrane was dried overnight at 25°C followed by blocking with 2% milk-PBS for 1 h. Immunoblotting was performed with ExtraAvidin Peroxidase Conjugate1:3000 (Sigma) and detection with ECL.

Aβ measurement

Brain cortical mitochondrial fractions and brain homogenates were incubated in 5 M guanidine HCl and 50 mM Tris HCl (pH 8.0) overnight and then subjected to Aβ concentration detection using human Aβ1-40 and Aβ1-42 ELISA kits (Invitrogen) following the manufacturer's instructions (7). For quantification of Aβ deposit, brain sections were cut from 4% paraformaldehyde-fixed brain and stained with antibody 3D6 (1:2000, provided by Eli Lilly, Indianapolis, IN, USA) to identify deposit. The area of plaque in the cortex from multiple sections at the same level in each experimental group was determined by image analysis using Universal Images software (Universal Imaging Corp., Downingtown, PA, USA).

Mitochondrial respiration assay

Mitochondrial oxygen consumption was measured as previously described by using a Clark electrode (8). A total of 100 μg mitochondria were resuspended in mitochondrial respiration buffer [225 mM mannitol, 75 mM sucrose, 2 mM K_2PO_4, 0.1% BSA, 5 mM glutamate]. The mitochondrial oxygen consumption was triggered by the addition of ADP (working concentration is 50 μM). The oxygen consumption rates at State III and State IV respiration were measured for data analysis.

Cytochrome c oxidase (CCO) activity assay

The CCO activity of mitochondrial fractions was measured using the CCO kit (Sigma). Briefly, a 60-μg mitochondria fraction and a suitable volume of enzyme dilution solution were added to 950 μl of assay buffer. The reaction was initiated by the addition of 50 μl of ferrocytochrome c substrate solution into the cuvette. The change in fluorescence at 550 nm was recorded immediately using a kinetic program with a 5-s delay, 10-s interval and total of six readings on an Ultrospect 3100 Pro spectrophotometer as previously described (7).

ATP levels

ATP levels were determined using an ATP Bioluminescence Assay Kit (Roche) following the manufacturer's instruction as we previously described (8,51). Briefly, the brain was quickly removed from anesthetic mice, slices of 1/4 cortex were immediately placed into liquid nitrogen, and then transferred to −80°C freezer until use. The slices of cortex were homogenized in the lysis buffer provided, incubated on ice for 30 min and centrifuged at 12 000*g* for 10 min. ATP levels were then measured in the subsequent supernatants using Luminescence plate reader (Molecular Devices). A 1.3 s delay time after substrate injection and 10 s integration time were used.

Evaluation of mitochondria and the intra-cellular ROS in Tg brain

Brain sections from Tg mice were stained with Mitosox-Red, a fluorochrome specific for anion superoxide produced in the inner mitochondrial compartment (Molecular Probes) for 30 min, and then images under confocal microscopy as described (8). Quantification of staining intensity and the percentage of area occupied by Mitosox were performed using Universal image program (8).

Evaluation of intra-cellular ROS levels was accessed by EPR spectroscopy as described in our previous study (52). CMH (cyclic hydroxylamine 1-hydroxy-3-methoxycarbonyl-2,2,5,5-tetramethyl-pyrrolidine) (100 μM) was incubated with hippocampal slices for 30 min, and then washed with cold PBS. The tissues were collected and homogenized with 100 μl of PBS for EPR measurement. The EPR spectra were collected, stored and analyzed with a Bruker EleXsys 540 x-band EPR spectrometer (Billerica, MA, USA) using the Bruker Software Xepr (Billerica, MA, USA).

Real-time PCR for measurement of cytokine and chemokines

Total RNA was extracted from cerebral cortices of Tg mice using TRIzol reagents (Invitrogen, Carlsbad, CA, USA) and was processed directly to produce cDNA using TaqMan reverse transcription reagents kit (Applied Biosystems, Foster City, CA, USA). Real-time PCR was utilized for quantification of gene expression of inflammatory mediator (IL-1β, TNF-α, MCP-1), microglial and monocyte markers (CD11b and CD4) and RAGE (receptor for advanced glycation end-product). The ribosomal RNA (18S) probes and primers were purchased from Applied Biosystems. Mouse RAGE primer and probe consist of forward primer, 5′-GGACCCTTAGCTGGCAC TTAGA-3′; reverse primer, 5′-GAGTCCCGTCTCAGGGTGTCT-3′ and probe (6FAM ATTCCCGATGGCAAAGAAACACTCGTG-TAMRA). Quantitative real-time PCR was performed using the ABI Prism 7900 Sequence Detection System (Applied Biosystems). Data are calculated using the $2^{-\Delta\Delta Ct}$ method as described by the manufacturer and are expressed as fold-increase over the indicated controls (1.0) in each figure.

Immunoblotting analysis

Samples were lysed in extraction buffer [10 mM Tris–HCl (pH 7.4), 100 mM sodium chloride, 1 mM EDTA, 1 mM EGTA, 1 mM sodium fluoride, 20 mM sodium pyrophosphate, 2 mM sodium orthovanadate, 1% Triton X-100, 10% glycerol, 0.1% SDS, 0.5% deoxycholate, 1 mM PMSF] containing protease inhibitor mixture (set V, EDTA-free; Calbiochem, San Diego, CA, USA), separated by SDS/PAGE (12% Bis–Tris gel; Invitrogen) and then transferred to a nitrocellulose membrane (Amersham, Pittsburgh, PA, USA). After blocking in TBST buffer (20 mM Tris–HCl, 150 mM sodium chloride, 0.1% Tween-20) containing 5% (wt/vol) nonfat dry milk (Santa Cruz) for 1 h at room temperature, the membrane was then incubated and gently shaken overnight (at 4°C) with

primary antibodies. This was followed by incubation with the corresponding secondary antibody for 1 h at room temperature. The following antibodies were used in this experiment: rabbit anti-PreP (1:4000, generated in our Lab), mouse anti-β actin (1:5000, Sigma, St. Louis, MO), goat anti-mouse IgG HRP conjugated and goat anti-rabbit IgG HRP conjugated (Invitrogen, Camarillo, CA, USA).

Electrophysiological studies

Electrophysiological recordings were performed on transverse hippocampal slices (400 μm in thickness), as described (8,24). The hippocampal slices were maintained in an interface chamber at 29°C and perfused with saline solution (124 mM NaCL, 4.4 mM KCL, 1 mM Na_2HPO_4, 25 mM $NaHCO_3$, 2 mM $CaCl_2$, 2.0 mM $MgSO_4$ and 10 mM glucose) continuously bubbled with 95% O_2 and 5% CO_2. Field-excitatory post-synaptic potential (fEPSPs) was recorded from the CA1 region of the hippocampus by placing both the stimulating and the recording electrodes in the CA1 stratum radiatum. The BST was assayed by plotting of the stimulus voltage (V) against slopes of fEPSP to generate input–output relations or by plotting of the peak amplitude of the fiber volley against the slope of the fEPSP to generate input–output relations. The LTP was induced using theta-burst stimulation (4 pulses at 100 Hz, with the bursts repeated at 5 Hz, and each tetanus, including three 10-burst trains separated by 15 s).

Behavioral test

Investigators were unaware of mouse genotypes until the behavioral tests were finished. The radial arm water maze test was performed as we previously described (8). The MWM test was performed according to the published method (53). The apparatus mainly compose a pool, which is 150 cm in diameter and 50 cm in height, a platform placed in one of the fixed quadrant for mice to escape, and a camera above the center of the pool to capture the images of the swimming mice. The tank is filled with water kept at 23 ± 2°C during the trials. The platform is hidden 0.5–1 cm below the water surface and the white paint was used to better cover the platform. In spatial acquisition session, mice were trained for six consecutive days with four trial each mouse per day. A trial started with releasing one mouse facing the pool wall and the mouse was allowed to swim freely and search for the escape platform. If the mouse cannot reach the platform within 60 s, it was guided to the platform and allowed to stay on for 15 s before the next trial. After all trials, mice were dried with paper towel and returned to its own cage. The escape latency was analyzed by the behavior software system (HVS water 2020). On the day 7, a probe trial was performed to assess the spatial memory of mice. The platform was removed from the pool and the mice were allowed to swim freely for 60 s. Traces of mice were recorded and data were analyzed by HVS water 2020.

Statistical analysis

One-way ANOVA was used for repeated measure analysis, followed by Fisher's protected least significant difference for post-hoc comparisons. $P < 0.05$ was considered significant. StatView statistics computer software was used. All data were expressed as the mean ± SEM.

Supplementary Material

Supplementary Material is available at *HMG* online.

Acknowledgement

We thank Molly Rabinowitz and Hung 'Key' Nguyen for assistance with mouse behavioral testing.

Conflict of Interest statement. None declared.

Funding

This study was supported by grants from the National Institute on Aging of the National Institutes of Health (NIH/NIA R37AG037319 and R01AG044793).

References

1. Lin, M.T. and Beal, M.F. (2006) Alzheimer's APP mangles mitochondria. *Nat. Med.*, **12**, 1241–1243.
2. Reddy, P.H. and Beal, M.F. (2008) Amyloid beta, mitochondrial dysfunction and synaptic damage: implications for cognitive decline in aging and Alzheimer's disease. *Trends Mol. Med.*, **14**, 45–53.
3. Yao, J., Irwin, R.W., Zhao, L., Nilsen, J., Hamilton, R.T. and Brinton, R.D. (2009) Mitochondrial bioenergetic deficit precedes Alzheimer's pathology in female mouse model of Alzheimer's disease. *Proc. Natl. Acad. Sci. USA*, **106**, 14670–14675.
4. Cardoso, S.M., Santos, S., Swerdlow, R.H. and Oliveira, C.R. (2001) Functional mitochondria are required for amyloid beta-mediated neurotoxicity. *FASEB J.*, **15**, 1439–1441.
5. Caspersen, C., Wang, N., Yao, J., Sosunov, A., Chen, X., Lustbader, J.W., Xu, H.W., Stern, D., McKhann, G. and Yan, S.D. (2005) Mitochondrial Abeta: a potential focal point for neuronal metabolic dysfunction in Alzheimer's disease. *FASEB J.*, **19**, 2040–2041.
6. Lustbader, J.W., Cirilli, M., Lin, C., Xu, H.W., Takuma, K., Wang, N., Caspersen, C., Chen, X., Pollak, S., Chaney, M. *et al.* (2004) ABAD directly links Abeta to mitochondrial toxicity in Alzheimer's disease. *Science*, **304**, 448–452.
7. Du, H., Guo, L., Yan, S., Sosunov, A.A., McKhann, G.M. and Yan, S.S. (2010) Early deficits in synaptic mitochondria in an Alzheimer's disease mouse model. *Proc. Natl. Acad. Sci. USA*, **107**, 18670–18675.
8. Du, H., Guo, L., Fang, F., Chen, D., Sosunov, A.A., McKhann, G. M., Yan, Y., Wang, C., Zhang, H., Molkentin, J.D. *et al.* (2008) Cyclophilin D deficiency attenuates mitochondrial and neuronal perturbation and ameliorates learning and memory in Alzheimer's disease. *Nat. Med.*, **14**, 1097–1105.
9. Wang, X., Su, B., Siedlak, S.L., Moreira, P.I., Fujioka, H., Wang, Y., Casadesus, G. and Zhu, X. (2008) Amyloid-beta overproduction causes abnormal mitochondrial dynamics via differential modulation of mitochondrial fission/fusion proteins. *Proc. Natl. Acad. Sci. USA*, **105**, 19318–19323.
10. Swerdlow, R.H. (2012) Mitochondria and cell bioenergetics: increasingly recognized components and a possible etiologic cause of Alzheimer's disease. *Antioxid. Redox. Signal*, **16**, 1434–1455.
11. Cha, M.Y., Han, S.H., Son, S.M., Hong, H.S., Choi, Y.J., Byun, J. and Mook-Jung, I. (2012) Mitochondria-specific accumulation of amyloid beta induces mitochondrial dysfunction leading to apoptotic cell death. *PloS One*, **7**, e34929.
12. Hansson Petersen, C.A., Alikhani, N., Behbahani, H., Wiehager, B., Pavlov, P.F., Alafuzoff, I., Leinonen, V., Ito, A., Winblad, B., Glaser, E. *et al.* (2008) The amyloid beta-peptide is imported into mitochondria via the TOM import machinery and localized to mitochondrial cristae. *Proc. Natl. Acad. Sci. USA*, **105**, 13145–13150.

13. Takuma, K., Fang, F., Zhang, W., Yan, S., Fukuzaki, E., Du, H., Sosunov, A., McKhann, G., Funatsu, Y., Nakamichi, N. *et al.* (2009) RAGE-mediated signaling contributes to intraneuronal transport of amyloid-beta and neuronal dysfunction. *Proc. Natl. Acad. Sci. USA*, **106**, 20021–20026.
14. Hedskog, L., Pinho, C.M., Filadi, R., Ronnback, A., Hertwig, L., Wiehager, B., Larssen, P., Gellhaar, S., Sandebring, A., Westerlund, M. *et al.* (2013) Modulation of the endoplasmic reticulum-mitochondria interface in Alzheimer's disease and related models. *Proc. Natl. Acad. Sci. USA*, **110**, 7916–7921.
15. Pavlov, P.F., Wiehager, B., Sakai, J., Frykman, S., Behbahani, H., Winblad, B. and Ankarcrona, M. (2011) Mitochondrial gamma-secretase participates in the metabolism of mitochondria-associated amyloid precursor protein. *FASEB J.*, **25**, 78–88.
16. Behbahani, H., Pavlov, P.F., Wiehager, B., Nishimura, T., Winblad, B. and Ankarcrona, M. (2010) Association of Omi/HtrA2 with gamma-secretase in mitochondria. *Neurochem. Int.*, **57**, 668–675.
17. Oddo, S., Caccamo, A., Shepherd, J.D., Murphy, M.P., Golde, T.E., Kayed, R., Metherate, R., Mattson, M.P., Akbari, Y. and LaFerla, F.M. (2003) Triple-transgenic model of Alzheimer's disease with plaques and tangles: intracellular Abeta and synaptic dysfunction. *Neuron*, **39**, 409–421.
18. Guo, L., Du, H., Yan, S., Wu, X., McKhann, G.M., Chen, J.X. and Yan, S.S. (2013) Cyclophilin D deficiency rescues axonal mitochondrial transport in Alzheimer's neurons. *PLoS One*, **8**, e54914.
19. Green, D.R., Galluzzi, L. and Kroemer, G. (2011) Mitochondria and the autophagy-inflammation-cell death axis in organismal aging. *Science*, **333**, 1109–1112.
20. Falkevall, A., Alikhani, N., Bhushan, S., Pavlov, P.F., Busch, K., Johnson, K.A., Eneqvist, T., Tjernberg, L., Ankarcrona, M. and Glaser, E. (2006) Degradation of the amyloid beta-protein by the novel mitochondrial peptidasome, PreP. *J. Biol. Chem.*, **281**, 29096–29104.
21. Stahl, A., Moberg, P., Ytterberg, J., Panfilov, O., Brockenhuus Von Lowenhielm, H., Nilsson, F. and Glaser, E. (2002) Isolation and identification of a novel mitochondrial metalloprotease (PreP) that degrades targeting presequences in plants. *J. Biol. Chem.*, **277**, 41931–41939.
22. Alikhani, N., Guo, L., Yan, S., Du, H., Pinho, C.M., Chen, J.X., Glaser, E. and Yan, S.S. (2011) Decreased proteolytic activity of the mitochondrial amyloid-beta degrading enzyme, PreP peptidasome, in Alzheimer's disease brain mitochondria. *J. Alzheimers Dis.*, **27**, 75–87.
23. Mucke, L., Masliah, E., Yu, G.Q., Mallory, M., Rockenstein, E.M., Tatsuno, G., Hu, K., Kholodenko, D., Johnson-Wood, K. and McConlogue, L. (2000) High-level neuronal expression of abeta 1–42 in wild-type human amyloid protein precursor transgenic mice: synaptotoxicity without plaque formation. *J. Neurosci.*, **20**, 4050–4058.
24. Arancio, O., Zhang, H.P., Chen, X., Lin, C., Trinchese, F., Puzzo, D., Liu, S., Hegde, A., Yan, S.F., Stern, A. *et al.* (2004) RAGE potentiates Abeta-induced perturbation of neuronal function in transgenic mice. *EMBO J.*, **23**, 4096–4105.
25. Takuma, K., Yao, J., Huang, J., Xu, H., Chen, X., Luddy, J., Trillat, A.C., Stern, D.M., Arancio, O. and Yan, S.S. (2005) ABAD enhances Abeta-induced cell stress *via* mitochondrial dysfunction. *FASEB J.*, **19**, 597–598.
26. Du, H., Guo, L., Zhang, W., Rydzewska, M. and Yan, S. (2011) Cyclophilin D deficiency improves mitochondrial function and learning/memory in aging Alzheimer disease mouse model. *Neurobiol. Aging*, **32**, 398–406.
27. Krysko, D.V., Agostinis, P., Krysko, O., Garg, A.D., Bachert, C., Lambrecht, B.N. and Vandenabeele, P. (2011) Emerging role of damage-associated molecular patterns derived from mitochondria in inflammation. *Trends Immunol.*, **32**, 157–164.
28. Fang, F., Lue, L.F., Yan, S., Xu, H., Luddy, J.S., Chen, D., Walker, D.G., Stern, D.M., Schmidt, A.M., Chen, J.X. *et al.* (2010) RAGE-dependent signaling in microglia contributes to neuroinflammation, Abeta accumulation, and impaired learning/memory in a mouse model of Alzheimer's disease. *FASEB J.*, **24**, 1043–1055.
29. Tillement, L., Lecanu, L., Yao, W., Greeson, J. and Papadopoulos, V. (2006) The spirostenol (22R, 25R)-20alpha-spirost-5-en-3beta-yl hexanoate blocks mitochondrial uptake of Abeta in neuronal cells and prevents Abeta-induced impairment of mitochondrial function. *Steroids*, **71**, 725–735.
30. Hansson, M.J., Mansson, R., Morota, S., Uchino, H., Kallur, T., Sumi, T., Ishii, N., Shimazu, M., Keep, M.F., Jegorov, A. *et al.* (2008) Calcium-induced generation of reactive oxygen species in brain mitochondria is mediated by permeability transition. *Free Radic. Biol. Med.*, **45**, 284–294.
31. Yao, J., Du, H., Yan, S., Fang, F., Wang, C., Lue, L.F., Guo, L., Chen, D., Stern, D.M., Gunn Moore, F.J. *et al.* (2011) Inhibition of amyloid-beta (Abeta) peptide-binding alcohol dehydrogenase-Abeta interaction reduces Abeta accumulation and improves mitochondrial function in a mouse model of Alzheimer's disease. *J. Neurosci.*, **31**, 2313–2320.
32. Du, H. and Yan, S.S. (2010) Mitochondrial permeability transition pore in Alzheimer's disease: cyclophilin D and amyloid beta. *Biochim. Biophys. Acta.*, **1802**, 198–204.
33. Calkins, M.J., Manczak, M., Mao, P., Shirendeb, U. and Reddy, P.H. (2011) Impaired mitochondrial biogenesis, defective axonal transport of mitochondria, abnormal mitochondrial dynamics and synaptic degeneration in a mouse model of Alzheimer's disease. *Hum. Mol. Genet.*, **20**, 4515–4529.
34. Manczak, M., Anekonda, T.S., Henson, E., Park, B.S., Quinn, J. and Reddy, P.H. (2006) Mitochondria are a direct site of A beta accumulation in Alzheimer's disease neurons: implications for free radical generation and oxidative damage in disease progression. *Hum. Mol. Genet.*, **15**, 1437–1449.
35. Zhu, X., Perry, G., Smith, M.A. and Wang, X. (2013) Abnormal mitochondrial dynamics in the pathogenesis of Alzheimer's disease. *J. Alzheimers Dis.*, **33** Suppl 1, S253–S262.
36. Reddy, P.H., Tripathi, R., Troung, Q., Tirumala, K., Reddy, T.P., Anekonda, V., Shirendeb, U.P., Calkins, M.J., Reddy, A.P., Mao, P. *et al.* (2012) Abnormal mitochondrial dynamics and synaptic degeneration as early events in Alzheimer's disease: implications to mitochondria-targeted antioxidant therapeutics. *Biochim. Biophys. Acta.*, **1822**, 639–649.
37. Wang, X., Su, B., Lee, H.G., Li, X., Perry, G., Smith, M.A. and Zhu, X. (2009) Impaired balance of mitochondrial fission and fusion in Alzheimer's disease. *J. Neurosci.*, **29**, 9090–9103.
38. Du, H., Guo, L., Wu, X., Sosunov, A.A., McKhann, G.M., Chen, J.X. and Yan, S.S. (2014) Cyclophilin D deficiency rescues Abeta-impaired PKA/CREB signaling and alleviates synaptic degeneration. *Biochim. Biophys. Acta.*, **1842**, 2517–2527.
39. Blomqvist, M.E., Chalmers, K., Andreasen, N., Bogdanovic, N., Wilcock, G.K., Cairns, N.J., Feuk, L., Brookes, A.J., Love, S., Blennow, K. *et al.* (2005) Sequence variants of IDE are associated with the extent of beta-amyloid deposition in the Alzheimer's disease brain. *Neurobiol. Aging*, **26**, 795–802.
40. Leissring, M.A., Farris, W., Wu, X., Christodoulou, D.C., Haigis, M.C., Guarente, L. and Selkoe, D.J. (2004) Alternative translation initiation generates a novel isoform of insulin-degrading enzyme targeted to mitochondria. *Biochem. J.*, **383**, 439–446.

41. Vangavaragu, J.R., Valasani, K.R., Gan, X. and Yan, S.S. (2014) Identification of human presequence protease (hPreP) agonists for the treatment of Alzheimer's disease. *Eur. J. Med. Chem.*, **76C**, 506–516.
42. Greenfield, J.P., Tsai, J., Gouras, G.K., Hai, B., Thinakaran, G., Checler, F., Sisodia, S.S., Greengard, P. and Xu, H. (1999) Endoplasmic reticulum and trans-Golgi network generate distinct populations of Alzheimer beta-amyloid peptides. *Proc. Natl. Acad. Sci. USA*, **96**, 742–747.
43. Cook, D.G., Forman, M.S., Sung, J.C., Leight, S., Kolson, D.L., Iwatsubo, T., Lee, V.M. and Doms, R.W. (1997) Alzheimer's A beta(1-42) is generated in the endoplasmic reticulum/intermediate compartment of NT2N cells. *Nat. Med.*, **3**, 1021–1023.
44. Hartmann, T., Bieger, S.C., Bruhl, B., Tienari, P.J., Ida, N., Allsop, D., Roberts, G.W., Masters, C.L., Dotti, C.G., Unsicker, K. *et al.* (1997) Distinct sites of intracellular production for Alzheimer's disease A beta40/42 amyloid peptides. *Nat. Med.*, **3**, 1016–1020.
45. Tienari, P.J., Ida, N., Ikonen, E., Simons, M., Weidemann, A., Multhaup, G., Masters, C.L., Dotti, C.G. and Beyreuther, K. (1997) Intracellular and secreted Alzheimer beta-amyloid species are generated by distinct mechanisms in cultured hippocampal neurons. *Proc. Natl. Acad. Sci. USA*, **94**, 4125–4130.
46. Wild-Bode, C., Yamazaki, T., Capell, A., Leimer, U., Steiner, H., Ihara, Y. and Haass, C. (1997) Intracellular generation and accumulation of amyloid beta-peptide terminating at amino acid 42. *J. Biol. Chem.*, **272**, 16085–16088.
47. Hagberg, H., Mallard, C., Rousset, C.I. and Thornton, C. (2014) Mitochondria: hub of injury responses in the developing brain. *Lancet Neurol.*, **13**, 217–232.
48. Origlia, N., Criscuolo, C., Arancio, O., Yan, S.S. and Domenici, L. (2014) RAGE inhibition in microglia prevents ischemia-dependent synaptic dysfunction in an amyloid-enriched environment. *J. Neurosci.*, **34**, 8749–8760.
49. Origlia, N., Bonadonna, C., Rosellini, A., Leznik, E., Arancio, O., Yan, S.S. and Domenici, L. (2010) Microglial receptor for advanced glycation end product-dependent signal pathway drives beta-amyloid-induced synaptic depression and long-term depression impairment in entorhinal cortex. *J. Neurosci.*, **30**, 11414–11425.
50. Dunkley, P.R., Jarvie, P.E. and Robinson, P.J. (2008) A rapid Percoll gradient procedure for preparation of synaptosomes. *Nat. Protoc.*, **3**, 1718–1728.
51. Huang, S., Wang, Y., Gan, X., Fang, D., Zhong, C., Wu, L., Hu, G., Sosunov, A.A., McKhann, G.M., Yu, H. *et al.* (2015) Drp1-mediated mitochondrial abnormalities link to synaptic injury in diabetes model. *Diabetes*, **64**, 1728–1742.
52. Gan, X., Wu, L., Huang, S., Zhong, C., Shi, H., Li, G., Yu, H., Howard Swerdlow, R., Xi Chen, J. and Yan, S.S. (2014) Oxidative stress-mediated activation of extracellular signal-regulated kinase contributes to mild cognitive impairment-related mitochondrial dysfunction. *Free Radic. Biol. Med.*, **75**, 230–240.
53. Vorhees, C.V. and Williams, M.T. (2006) Morris water maze: procedures for assessing spatial and related forms of learning and memory. *Nat. Protoc.*, **1**, 848–858.